

Sb lattice diffusion in $\text{Si}_{1-x}\text{Ge}_x/\text{Si}(001)$ heterostructures: Chemical and stress effectsA. Portavoce,^{1,2} P. Gas,² I. Berbezier,¹ A. Ronda,¹ J. S. Christensen,³ A. Yu. Kuznetsov,³ and B. G. Svensson³
¹CRMC2-CNRS, Campus de Luminy, Case 913, 13288 Marseille Cedex 9, France²L2MP-CNRS, Av. escadrille Normandie-Niemen, Case 151, 13397 Marseille Cedex 13, France³Royal Institute of Technology (KTH), Department of Electronics, Electrum 229, SE-164 40 Kista-Stockholm, Sweden

(Received 7 March 2003; revised manuscript received 3 September 2003; published 15 April 2004)

The Sb diffusion coefficient in $\text{Si}_{1-x}\text{Ge}_x/\text{Si}_{1-y}\text{Ge}_y(001)$ heterostructures grown by molecular beam epitaxy (MBE) was measured for temperatures ranging from 700 to 850 °C, Ge composition from 0 to 20 % and biaxial pressure from -0.8 (tension) to 1.4 GPa (compression). A quantitative separation of composition and biaxial stress effects is made. We show that the Sb lattice diffusion coefficient: (i) increases with Ge concentration in relaxed layers or at constant biaxial pressure and (ii) increases with compressive biaxial stress and decreases with tensile biaxial stress at constant Ge composition. The enhancement of Sb lattice diffusion in $\text{Si}_{1-x}\text{Ge}_x$ layers in epitaxy on Si(001) is thus due to the cooperative effect of Ge composition and induced compressive biaxial stress. However, the first effect (composition) is predominant. The activation volume of Sb diffusion in $\text{Si}_{1-x}\text{Ge}_x$ layers is deduced from the variation of the Sb diffusion coefficients with biaxial pressure. This volume is negative. The sign of the activation volume, its absolute value and its variation with temperature confirm the prediction of the thermodynamic model proposed by Aziz, namely, that under a biaxial stress the activation volume is reduced to the relaxation volume.

DOI: 10.1103/PhysRevB.69.155415

PACS number(s): 68.55.Ln, 66.30.Jt, 66.30.Pa

I. INTRODUCTION

The control of doping profiles of Si-based heterostructures is crucial for the fabrication of microelectronic or optoelectronic devices. Key issues are the realization of sharp (δ) profiles, of locally (highly) doped epilayers and/or nanostructures.¹ To produce such structures, there is a strong need to understand and control dopant redistribution phenomena. There are several difficulties to overcome. The first one is that dopant redistribution already takes place during molecular beam epitaxy (MBE) or chemical vapor deposition (CVD) growth² and is thus controlled both by thermodynamics (e.g., segregation enthalpy) and kinetics (e.g., growth rate, near surface exchanges). The second one is that heterostructures consist of epitaxied layers with different compositions and levels of stress. These two parameters are linked. A modification of the Ge content (x) of a $\text{Si}/\text{Si}_{1-x}\text{Ge}_x$ heterostructure will induce (i) an intrinsic “alloying” effect due to Si-Ge substitution and (ii) a stress effect due to the evolution of the $\text{Si}/\text{Si}_{1-x}\text{Ge}_x$ lattice mismatch.

The goal of this paper is to separate the influence of these two effects in the case of lattice diffusion. From a practical point of view, lattice diffusion is a secondary redistribution process during the growth of heterostructures, its role is, however, important for subsequent annealing steps for which it becomes the main redistribution mechanism. Moreover, because of its “relative” simplicity and its close link to defect properties, the understanding of lattice diffusion appears as a useful step in the analysis of more complex redistribution processes such as segregation during growth.³

On the other hand, the analysis of lattice diffusion in $\text{Si}/\text{Si}_{1-x}\text{Ge}_x$ heterostructures presents several fundamental interests.

(1) MBE allows the synthesis of a large variety of $\text{Si}_{1-x}\text{Ge}_x$ layers with different Ge concentration and stress states. By using different relaxed buffers it is possible to

modulate for the same Ge composition the stress state from tension to compression.

(2) The modifications of the diffusion coefficients induced by composition and pressure changes are useful for the analysis of diffusion mechanisms.⁴

(3) The stress created by epitaxy is biaxial (and not hydrostatic), a situation which is frequently encountered in microelectronic structures but has not received as much attention (as far as diffusion mechanisms are concerned) as hydrostatic pressure.

The dopant studied is Sb, which is the typical n -type dopant used for the MBE growth of Si-based heterostructures. Its diffusion in silicon (and silicon-germanium alloys) has been extensively studied, and it is established that its diffusion mechanism is mainly controlled by vacancies.^{4,5} The effect of hydrostatic pressure is to decrease the Sb lattice diffusion coefficient.^{6,7} Concerning $\text{Si}/\text{Si}_{1-x}\text{Ge}_x$ heterostructures it has been shown that the Sb lattice diffusion: (i) increases with Ge composition (x) in compressively strained or relaxed $\text{Si}_{1-x}\text{Ge}_x$ layers^{8,9} and (ii) increases in a compressively strained $\text{Si}_{0.91}\text{Ge}_{0.09}$ layer and decreases in a Si layer under tensile strain.¹⁰ A formalism has been developed by Aziz to analyze the thermodynamics of diffusion under hydrostatic pressure and biaxial stress and the relation to point defect mechanisms.¹¹

In this paper, we measure the lattice diffusion coefficient of antimony (Sb) in $\text{Si}_{1-x}\text{Ge}_x$ layers with different compositions ($0 \leq x < 0.2$) and stress states. The influence of composition and stress is differentiated. We show that Sb diffusion coefficient: (i) increases with Ge composition at constant biaxial stress and (ii) increases under biaxial compressive stress and decreases under biaxial tensile stress at constant Ge composition. The activation volume of diffusion and its variation with temperature and composition are deduced from the variations with stress. Its value (negative) and its variations confirm the prediction of the model developed by

Aziz and the statement that under biaxial stress the activation volume depends mainly on the volume of relaxation.¹¹ That explains the different diffusion behavior observed under hydrostatic and biaxial compression.

II. EXPERIMENT

$\text{Si}_{1-x}\text{Ge}_x/\text{Si}_{1-y}\text{Ge}_y(001)$ structures were grown in a Riber MBE system with a base pressure of typically $\sim 10^{-11}$ Torr. Silicon was evaporated from a floating zone silicon crystal using an electron gun. Germanium and antimony were evaporated from effusion Knudsen cells. Phosphorous-doped Si(001) wafers of nominal orientation (miscut $< 0.1^\circ$) were used as substrates. They were first cleaned and protected by an oxide layer using standard chemical process. After introduction in the growth chamber, a 900°C annealing was performed to dissociate the surface oxide. A 50-nm-thick Si buffer layer was then grown on the substrates at 750°C to achieve a reproducible initial Si surface; its quality was checked by the RHEED intensity of the (2×1) reconstruction.

Three types of heterostructures were grown in order to obtain (i) relaxed $\text{Si}_{1-x}\text{Ge}_x$ layers (with $x=0, 0.09, 0.18$), (ii) compressively strained $\text{Si}_{1-x}\text{Ge}_x$ layers ($x=0.03, 0.07, 0.09, 0.15, 0.18$), and (iii) tensively strained $\text{Si}_{1-x}\text{Ge}_x$ layers ($x=0.09, 0.18$). Details and schematic representations of these heterostructures can be found in Ref. 3. They consist of a stack of four layers: (a) a 50-nm-thick $\text{Si}_{1-x}\text{Ge}_x$ layer deposited at 650°C , (b) a half monolayer of Sb deposited at 400°C , (c) a 6-nm-thick $\text{Si}_{1-x}\text{Ge}_x$ layer deposited at 200°C , and (d) a 45-nm-thick $\text{Si}_{1-x}\text{Ge}_x$ layer deposited at 550°C . Layer (c) was grown at low temperature (200°C) in order to bury as much as possible the Sb layer. Its crystallographic quality was restored by a 5-min anneal before deposition of layer (d), respectively at 750°C for the strained structures and at 600°C for the relaxed ones in order to limit dislocations propagation. (e) A 20-nm-thick Si cap grown at $T < 200^\circ\text{C}$ was deposited on top of the compressively strained structures.

This stack of layers was deposited on a Si(001) substrate to produce compressively strained layers, on a relaxed buffer with the same Ge composition in order to obtain relaxed layers, or on a relaxed buffer with a higher Ge concentration to produce layers under tensile strain (a $\text{Si}_{0.81}\text{Ge}_{0.19}$ buffer and a $\text{Si}_{0.78}\text{Ge}_{0.22}$ buffer were used to strain, respectively, the $\text{Si}_{0.91}\text{Ge}_{0.09}$ layer and the $\text{Si}_{0.82}\text{Ge}_{0.18}$ layer). Figure 1 illustrates the case of a $\text{Si}_{0.91}\text{Ge}_{0.09}$ layer in epitaxy on a relaxed $\text{Si}_{0.81}\text{Ge}_{0.19}$ buffer.

The relaxed buffers were obtained by the successive deposition of (i) a 100-nm-thick Si layer grown at 400°C , (ii) a 700-nm-thick $\text{Si}_{1-x}\text{Ge}_x$ layer grown at 550°C . This technique allows the glide of the majority of the threading dislocations in the low temperature Si layer.^{12,13} This is demonstrated in Fig. 2. The concentration of dislocations in these $\text{Si}_{1-x}\text{Ge}_x$ buffers was measured by atomic force microscopy and transmission electron microscopy. It was found lower than 10^5 cm^{-2} . X-ray diffraction measurements confirmed that the level of relaxation in the buffers was larger than 95%. The concentration of Ge (x) in these heterostructures

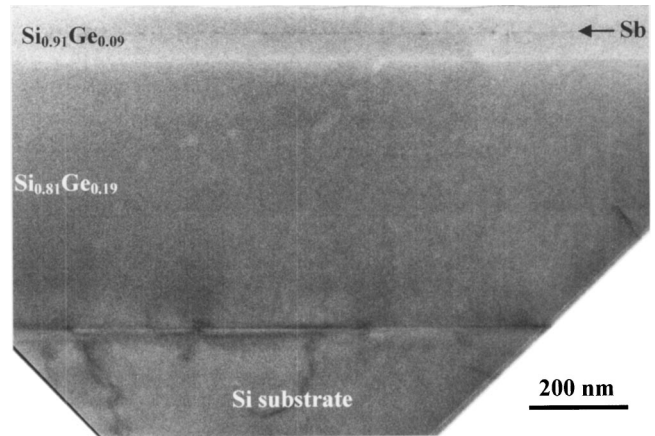


FIG. 1. TEM cross-section view of a $\text{Si}_{0.91}\text{Ge}_{0.09}$ layer tensely strained on a $\text{Si}_{0.81}\text{Ge}_{0.19}$ relaxed buffer. The dislocation density in the tensely strained layer measured by AFM and TEM in plan view is equal to $2.5 \times 10^4 \text{ disloc/cm}^2$.

was checked by Rutherford backscattering spectrometry (RBS).

After growth, each sample was cleaved in several pieces, one of them was kept as a reference and the others were annealed at different temperatures ($700 < T < 900^\circ\text{C}$) in a vacuum furnace ($P \sim 10^{-6}$ Torr). Annealing times ($1 \text{ h} < t < 8$ days) were chosen such that the mean penetration depth (\sqrt{Dt}) remains in the range of 5 to 10 nm whatever the annealing temperature. At a given temperature, samples of different compositions and stress states were annealed together in order to minimize experimental uncertainties. The profiles of Sb concentration versus depth were measured by secondary ion mass spectrometry (SIMS) using a Cameca IMS4F operated at 8 Kev under O_2^+ primary ions. The corresponding profiles before and after anneal were measured in the same run. The Sb lattice diffusion coefficient was then deduced from a comparison between the Sb distribution measured after annealing and a numerical fit of the diffusion equation using the before-anneal profile as initial distribution.¹⁴ Figure 3 illustrates this effect in the case of Sb diffusion in a pure silicon layer after annealing at 850°C during 10 h. The fit, based on a diffusion coefficient equal to $7.8 \times 10^{-17} \text{ cm}^2/\text{s}$, is correct except in the tail of the distri-

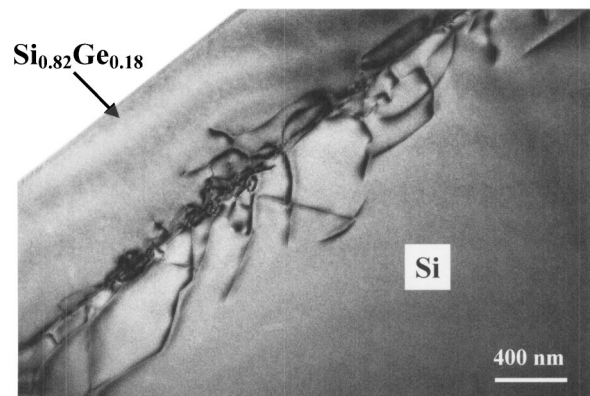


FIG. 2. TEM cross-section view of a relaxed $\text{Si}_{0.82}\text{Ge}_{0.18}$ buffer.

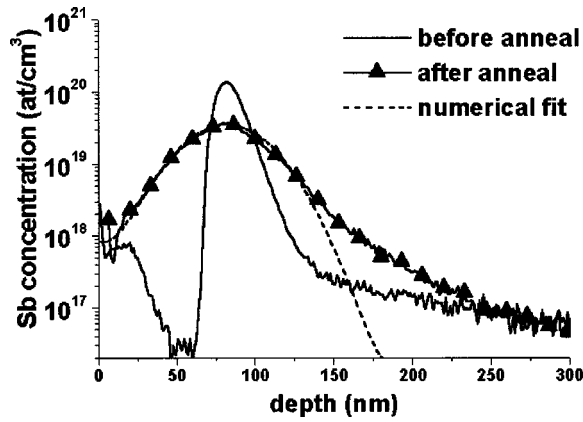


FIG. 3. Sb depth profiles in Si before and after an anneal at 850 °C for 10 h. Comparison of the profile obtained after annealing and a fit based on the initial profile and a diffusion coefficient equal to $7.8 \times 10^{-17} \text{ cm}^2/\text{s}$.

bution. This tail is mainly a SIMS artifact due to the ion bombardment, the total decay length of this tail being equal to the sum of the real decay length of the dopant profile and the beam-induced decay length.¹⁵ Due to this SIMS artifact (right part of the profiles), the simulated profiles were considered correct when they fitted in the best way the left part of the SIMS profiles.

III. RESULTS

The growth of the low temperature layer (c) allowed a high incorporation of Sb. This high incorporation level may induce the formation of Sb clusters. This was observed in the $\text{Si}_{1-x}\text{Ge}_x$ layers ($0.03 \leq x \leq 0.18$) but not in the pure Si ones, which is most likely a consequence of the higher Sb solubility limit in Si (0.1 at. %) than in Ge (0.035 at. %).¹⁶

Figure 4 presents a high resolution TEM cross-section view showing the presence of Sb clusters in a $\text{Si}_{0.91}\text{Ge}_{0.09}$ layer. Figure 5 illustrates the influence of these Sb clusters on the redistribution profiles. One can notice that there is no Sb transport for Sb concentration higher than $\sim 2\text{--}3 \times 10^{19} \text{ at/cm}^3$ ($\sim 0.04\text{--}0.06$ at. %). This value constitutes thus an estimation of the Sb solubility limit. This effect was taken into account in the calculation of the Sb diffusion coefficient using a parameter (S_i) corresponding to the concentration limit above which Sb atoms did not diffuse during annealing. S_i was determined for each simulation and was found to be in the range of 2 to $3 \times 10^{19} \text{ at/cm}^3$. Such a result means that the cluster acts as a source for diffusion: the concentration at the cluster/ $\text{Si}_{1-x}\text{Ge}_x$ interface stays constant during the heat treatment. Tables I(a), I(b), and I(c) give the Sb diffusion

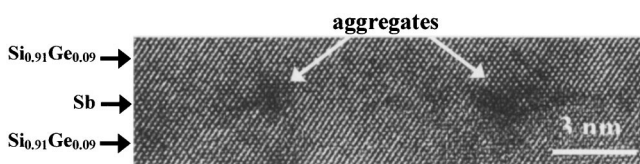


FIG. 4. High-resolution TEM cross-section view of Sb clusters in a $\text{Si}_{0.91}\text{Ge}_{0.09}$ layer.

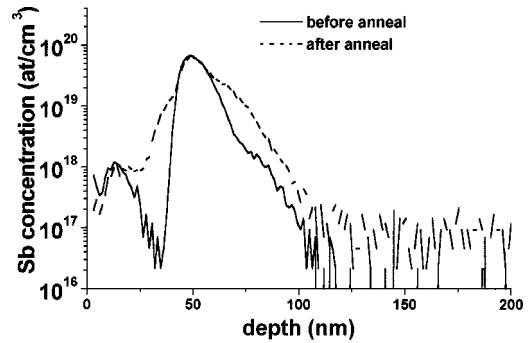


FIG. 5. Sb depth profiles in a $\text{Si}_{0.93}\text{Ge}_{0.07}$ layer before and after an anneal at 750 °C for 35 h: influence of the formation of Sb clusters on the diffusion profile.

coefficients measured for temperatures ranging from 700–900 °C in $\text{Si}_{1-x}\text{Ge}_x$ layers ($0 \leq x \leq 0.18$) respectively under biaxial compression, no stress (relaxed), or under biaxial tension.

A. Influence of the Ge concentration in $\text{Si}_{1-x}\text{Ge}_x$ layers in epitaxy on Si(001) substrate, joint effect of Ge composition, and induced stress

Figure 6 shows the evolution of the Sb diffusion coefficient versus the Ge concentration (x) in $\text{Si}_{1-x}\text{Ge}_x$ layers in epitaxy on Si(001) substrates for different temperatures. One can notice the following.

(1) The diffusion coefficient measured in pure Si layers is slightly higher than that obtained from the extrapolation (at $x=0$) of the diffusion coefficients in $\text{Si}_{1-x}\text{Ge}_x$ layers. This is very likely the consequence of a charge effect. Sb diffusion in Si and Ge proceeds via neutral vacancies. However, when the doping level is increased, charged defects (e.g., singly charged vacancies) will contribute to the diffusion process.^{2,3} The importance of this enhancement is, as a first approximation, proportional to the ratio (n/n_i) between the Sb doping level (n) and the intrinsic carrier concentration (n_i).^{4,17} Because of the formation of Sb clusters, the effective doping level reached in the $\text{Si}_{1-x}\text{Ge}_x$ layers ($\sim 10^{19} \text{ at/cm}^3$) is lower than in the pure Si ones ($\sim 10^{20} \text{ at/cm}^3$). Moreover the intrinsic carrier concentration is higher in $\text{Si}_{1-x}\text{Ge}_x$ than in Si at constant temperature. Consequently, at $T=800$ °C, the ratio n/n_i is ~ 166 for the pure Si layer, ~ 9 for the $\text{Si}_{0.97}\text{Ge}_{0.03}$ one, and ~ 3 for the most Ge concentrated layer ($\text{Si}_{0.82}\text{Ge}_{0.18}$). This shows that the contribution of charged defects to diffusion in the pure Si layers is more than one order of magnitude larger than in the Ge alloyed layers, while it is slightly different between the $\text{Si}_{1-x}\text{Ge}_x$ layers (in the range of concentration studied).

(2) The Sb diffusion coefficient increases when the Ge concentration increases. The values measured as well as the concentration dependence are consistent with that previously reported for $\text{Si}_{1-x}\text{Ge}_x$ layers in epitaxy on Si(001) substrates.⁸ Consistent with this increase of the diffusion coefficient, the activation energies decrease with Ge concentration. They range from $\sim 3.5 \pm 0.5 \text{ eV}$ ($\text{Si}_{0.97}\text{Ge}_{0.03}$) to $\sim 3 \pm 0.2 \text{ eV}$ ($\text{Si}_{0.82}\text{Ge}_{0.18}$). These values are lower than those

TABLE I. (a) Sb lattice diffusion coefficients (D cm²/s) measured in Si_{1-x}Ge_x layers in compression [epitaxy on Si(100)]. (b) Sb lattice diffusion coefficients (D cm²/s) measured in relaxed Si_{1-x}Ge_x layers (epitaxy on a relaxed Si_{1-x}Ge_x buffer). (c) Sb lattice diffusion coefficients (D cm²/s) measured in Si_{1-x}Ge_x layers in tension (epitaxy on a relaxed Si_{1-y}Ge_y buffer with $y > x$).

(a)						
$T(^{\circ}\text{C})$	$x=0$	$x=0.03$	$x=0.07$	$x=0.09$	$x=0.15$	$x=0.18$
700			3.8×10^{-19}	8.8×10^{-19}	1.4×10^{-18}	5.5×10^{-18}
750	1.7×10^{-18}	1.1×10^{-18}	2.7×10^{-18}	3.8×10^{-18}	8.8×10^{-18}	1.3×10^{-17}
800	8.6×10^{-18}	1.0×10^{-17}	2.0×10^{-17}	6.3×10^{-17}	1.1×10^{-16}	1.4×10^{-16}
850	7.8×10^{-17}	4.1×10^{-17}	7.2×10^{-17}	9.5×10^{-17}	2.8×10^{-16}	
900	2.3×10^{-16}	2.0×10^{-16}				

(b)		
$T(^{\circ}\text{C})$	$x=0.09$	$x=0.18$
700	5.9×10^{-19}	1.3×10^{-18}
750	3.6×10^{-18}	4.5×10^{-18}
800	4.8×10^{-17}	5.2×10^{-17}
850	1.5×10^{-16}	

(c)		
$T(^{\circ}\text{C})$	$x=0.09$	$x=0.18$
700	4.4×10^{-19}	8.5×10^{-19}
750	3.6×10^{-18}	4.3×10^{-18}
800	3.8×10^{-17}	4.9×10^{-17}
850	1.3×10^{-16}	

obtained in Ref. 8 (ranging from 4.08 ± 0.07 to 3.85 ± 0.12 eV). Such discrepancies can be explained by the error bar on the coefficients of diffusion and by the very small temperature ranges studied: $\Delta T = 100^{\circ}\text{C}$ in Ref. 8 and 150°C in this study. These two points induce large uncertainty on the activation energy. Such discrepancies are not exceptional for diffusion studies in Si.^{4,5}

B. Influence of stress at constant Ge composition

Figures 7(a) and 7(b) give the variation of the Sb diffusion coefficient as a function of biaxial pressure at constant

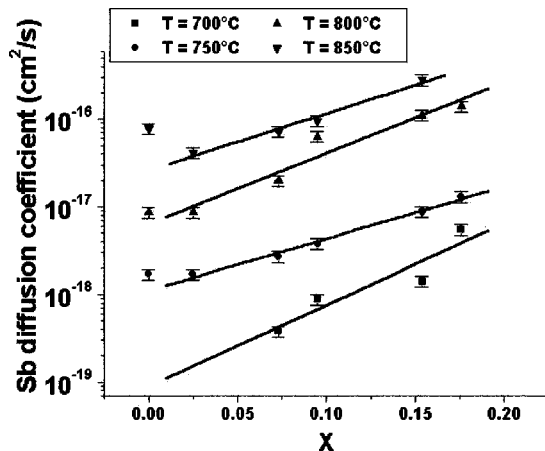


FIG. 6. Variation of the Sb lattice diffusion coefficients with Ge concentration (x) in Si_{1-x}Ge_x layers grown in epitaxy on Si(001) substrates.

temperature (700 and 800 °C) and for two different Ge compositions (Si_{0.91}Ge_{0.09} and Si_{0.82}Ge_{0.18}). The biaxial pressure (p^b) has been calculated from the following equation valid for a film in epitaxy on a substrate:^{18,19}

$$p^b = 2\mu \frac{\nu + 1}{\nu - 1} \left(\frac{a_{\text{film}} - a_{\text{sub}}}{a_{\text{sub}}} \right). \quad (1)$$

In this equation, a_{film} , μ , and ν are, respectively, the unconstrained lattice parameter, the shear modulus, and the Poisson ratio of the film, a_{sub} is the lattice parameter of the substrate (buffer). This equation gives positive pressures for biaxial compression and negative pressures for biaxial tension. It clearly appears that the Sb diffusion coefficient increases with a biaxial compression and decreases with a biaxial tension, which is consistent with the results presented in Ref. 10.

C. Influence of the Ge composition at constant stress

Figure 8 gives the variation of the Sb diffusion coefficient in Si_{1-x}Ge_x layers as a function of Ge composition for three biaxial pressures (-0.3, 0, and +0.6 Gpa) at 700 °C. The values reported are directly deduced from the fits of the diffusion coefficients versus biaxial pressure presented in Figs. 7(a) and 7(b). One can notice that for relaxed layers as well as for layers under constant compressive or tensile stress the Sb diffusion coefficient increases with Ge composition.

IV. DISCUSSION

The separation between the influence of chemistry (Ge composition) and epitaxial stress allows a better analysis of

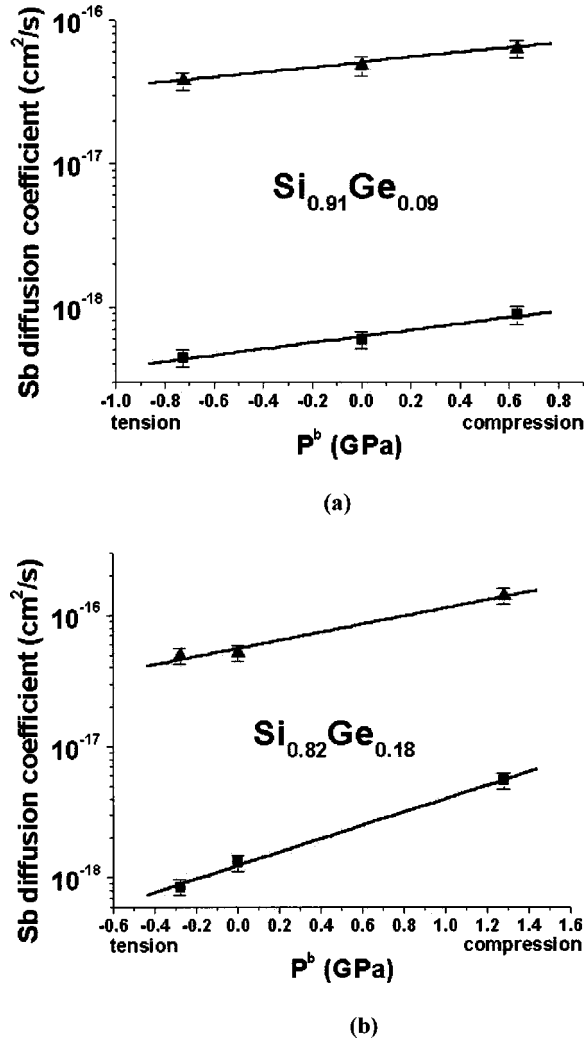


FIG. 7. Variation of the Sb lattice diffusion coefficients at 700 (■) and 800 °C (▲) with biaxial pressure in (a) $\text{Si}_{0.91}\text{Ge}_{0.09}$ and (b) $\text{Si}_{0.82}\text{Ge}_{0.18}$ layers.

the Sb diffusion in $\text{Si}_{1-x}\text{Ge}_x$ layers. Our results show that for $\text{Si}/\text{Si}_{1-x}\text{Ge}_x$ heterostructures the observed increase in the antimony diffusion coefficient (D) is due to the additive contribution of chemistry (Ge composition) and compressive stress. However, the amplitude of these two contributions is different, the main contribution to the enhancement being chemistry. For example, at 800 °C the addition of 9% Ge to Si induces a global increase of the Sb diffusion coefficient by a factor of ~ 7 ($D_{\text{Si}_{0.91}\text{Ge}_{0.09} \text{ comp}}/D_{\text{Si}} = 6.3 \times 10^{-17}/8.6 \times 10^{-18}$). This factor can be subdivided in ~ 5.65 ($D_{\text{Si}_{0.91}\text{Ge}_{0.09} \text{ relaxed}}/D_{\text{Si}} = 4.8 \times 10^{-17}/8.6 \times 10^{-18}$) for chemistry and ~ 1.35 ($D_{\text{Si}_{0.91}\text{Ge}_{0.09} \text{ comp}}/D_{\text{Si}_{0.91}\text{Ge}_{0.09} \text{ relaxed}} = 6.3 \times 10^{-17}/4.8 \times 10^{-17}$) for compressive stress.

A. Influence of chemistry (Ge composition)

In relaxed structures and at constant biaxial pressure, the Sb diffusion coefficient increases with Ge composition. This “chemical” effect is easily understood if one considers the Sb diffusion mechanisms in Si and Ge. It is established that

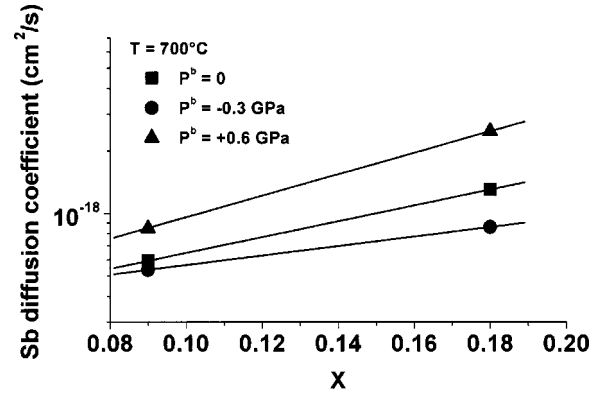


FIG. 8. Variation at 700 °C of the Sb lattice diffusion coefficients with Ge composition for $\text{Si}_{1-x}\text{Ge}_x$ layers under different biaxial pressures -0.3 (tension), 0 (relaxed), and $+0.6$ Gpa (compression).

in both semiconductors, Sb diffuses preferentially via vacancies.^{4,5} Moreover, at fixed temperature, the diffusion of Sb in Ge is several orders of magnitude larger than in Si due to a larger vacancy concentration in accordance with the “melting point rule” which states that in closely related crystals, point defect formation energies scale with melting temperatures.²⁰ The increase of the Sb diffusion coefficient is thus consistent with a vacancy mechanism and an enhancement of the vacancy concentration linked to Ge addition. This also agrees with the observed decrease of the activation energies with the increase of Ge concentration.

B. Influence of biaxial stress

At constant Ge concentration, the Sb diffusion coefficient increases with biaxial compressive stress and decreases with biaxial tensile stress. These variations can be used to quantitatively analyze the effect of a biaxial pressure on Sb diffusion through the activation volume (ΔV):

$$\Delta V = \left(\frac{dG}{dP} \right)_T, \quad (2)$$

where G is the Gibbs energy of diffusion, P the pressure, and T the temperature.

The subdivision of the Gibbs energy of diffusion into the free energy of formation and migration leads to a splitting of the activation volume according to

$$\Delta V = \Delta V^f + \Delta V^m, \quad (3)$$

where ΔV^f and ΔV^m are the formation and migration volumes of the intrinsic defect controlling diffusion (here a vacancy). The migration volume can be understood as the variation of the relaxation volume during the defect motion. Providing diffusion takes place via a single diffusion mechanism, the activation volume can be obtained from the variations of D as a function of the pressure:^{4,5}

$$\Delta V = -kT \frac{d \ln D}{dP}, \quad (4)$$

TABLE II. Volume of activation at 700 and 800 °C for Sb diffusion in $\text{Si}_{0.91}\text{Ge}_{0.09}$ and $\text{Si}_{0.82}\text{Ge}_{0.18}$ layers. The volume of activation is expressed in function of the atomic volume (Ω).

$T(^{\circ}\text{C})$	$x=0.09$	$x=0.18$
700	-0.34Ω	-0.77Ω
800	-0.28Ω	-0.51Ω

where k is the Boltzmann constant. The values deduced from Figs. 7(a) and 7(b) are reported in Table II. One observes that ΔV is negative. It is expected that for a vacancy mechanism^{6,7,20–22} under hydrostatic pressure, the activation volume for Sb diffusion in Si is positive.

This negative value of the activation volume for Sb diffusion under biaxial stress agrees with theoretical predictions from Aziz who analyzed the thermodynamics of diffusion under hydrostatic pressure and biaxial stress.^{11,23} Equations (10) and (11) of Ref. 23 show that the expression of the activation volume under hydrostatic pressure is

$$\Delta V^h = \Omega + V^r + V^m. \quad (5)$$

while under biaxial pressure

$$\Delta V^b = 2/3 V^r + V^m - V_{\parallel}^m. \quad (6)$$

In these expressions, Ω is the atomic volume [(+) for a vacancy and (–) for an interstitial], V^r the relaxation volume, V^m the trace of the migration volume tensor, V_{\parallel}^m (V_{\perp}^m) its components in the direction parallel (respectively, perpendicular) to the direction of diffusion. If one assumes that the volume of the defect is constant, which means that lattice distortions are in the elastic regime, and that each direction has a constant elasticity then $V_{\perp}^m = 0$ and $V_{\parallel}^m = 0$ leading to $\Delta V^m = 0$. This is equivalent to neglect the migration part in the activation volume. Within this approximation, and assuming that for a vacancy^{23–25}

$$V^r \leq 0 \quad \text{and} \quad \Omega \geq |V^r| \quad (7)$$

the activation volume is found positive for an hydrostatic pressure

$$\Delta V^h \sim \Omega + V^r \quad (8)$$

and negative for biaxial stress

$$\Delta V^b \sim 2/3 V^r. \quad (9)$$

The latter result is explained by the fact that under biaxial pressure the activation volume contains only the relaxation part. Using expressions (8), (9) and the value of ΔV^h measured by Zhao *et al.*⁷ for Sb diffusion in Si under hydrostatic pressure ($\Delta V^h = 0.07 \Omega \pm 0.02 \Omega$ at 860 °C) one finds $V^r \sim -0.93 \Omega$ and $\Delta V^b \sim -0.62 \Omega$ a value which can be compared to the value of activation volumes under biaxial pressure determined in this study and reported in Table II.

It is also interesting to mention that in the case of Ge self-diffusion (vacancy mechanism) under hydrostatic pressure Werner *et al.*²⁶ have measured $\Delta V^h = +0.24 \Omega$ at 600 °C and $\Delta V^h = +0.41 \Omega$ at 813 °C. These values lead (using the same assumptions: $\Delta V^m \sim 0$) to $V^r \sim -0.76 \Omega$ at 600 °C and $V^r \sim -0.59 \Omega$ at 813 °C. These variations of the relaxation volume with temperature are similar to the one we observed for the activation volume under biaxial pressure (Table II) giving additional support to the conclusion that this volume includes mainly a relaxation part.

V. CONCLUSION

The use of MBE made $\text{Si}_{1-x}\text{Ge}_x/\text{Si}_{1-y}\text{Ge}_y(001)$ heterostructures allowed us to study Sb lattice diffusion in $\text{Si}_{1-x}\text{Ge}_x$ layers with different Ge composition and stress states. The Sb diffusion coefficient was measured for temperature ranging from 700 to 850 °C, Ge composition from 0 to 20% and biaxial pressure from -0.8 (tension) to 1.4 GPa (compression).

We show that (1) in relaxed layers or for constant biaxial (tensile or compressive) pressure, the Sb lattice diffusion coefficient increases with Ge concentration. This is consistent with the fact that in both semiconductors Sb diffusion is vacancy mediated. (2) At constant Ge composition, the Sb diffusion coefficient increases with compressive biaxial stress and decreases with tensile biaxial stress. (3) It results from points (1) and (2) that the enhancement of Sb lattice diffusion in $\text{Si}_{1-x}\text{Ge}_x$ layers in epitaxy on Si(001) is due to the cooperative effect of Ge concentration and induced compressive biaxial stress. However, the first factor (chemistry) is predominant. (4) The activation volume of Sb diffusion in $\text{Si}_{1-x}\text{Ge}_x$ layers has been deduced from the variation of the Sb diffusion coefficients with biaxial pressure. This volume is negative while it is positive for diffusion under hydrostatic pressure. The negative sign of the activation volume as well as its absolute value and its variation with temperature confirm the prediction of the thermodynamic model proposed by Aziz, namely, that under hydrostatic pressure the activation volume is the sum of the volume of formation and relaxation while under a biaxial stress the activation volume is reduced to the relaxation volume. This explains why for a same diffusion mechanism a biaxial compression and a hydrostatic pressure have opposite effects on mass transport.

ACKNOWLEDGMENTS

Our understanding of these diffusion problems would not be the same without regular discussion with several colleagues. Let us thank, C. Girardeaux, F. M. d'Heurle, M. Lannoo, D. Manginck, J. Parret, J. Philibert, and G. Treglia for their advice and comments. Financial support by EC through Contract Nos. FORUM-FIB (IST-2000-29573) and SIGENET (HPRN-CT-1999-0123) is acknowledged.

- ¹*Proceedings of the Eighth International Conference on the Electronic Properties of Two-Dimensional Systems*, edited by J. Y. Marzin, Y. Guldner, and J. C. Maan [Surf. Sci. **229** (1990)].
- ²S. Andrieu, F. Amaud d'Avitaya, and J. C. Pliester, J. Appl. Phys. **65**, 2681 (1989), and references therein.
- ³A. Portavoce, I. Berbezier, P. Gas, and A. Ronda, Phys. Rev. B (to be published).
- ⁴N. A. Stolwijk and H. Bracht, *Landolt-Bornstein-Numerical Data and Functional Relationships in Science and Technology*, edited by D. Beke (Springer-Verlag, Berlin, 1998), Vol. III-33A, p. 2-1.
- ⁵W. Frank, U. Gosele, H. Mehrer, and A. Seeger, *Diffusion in Crystalline Solids* (Academic Press, New York, 1984), p. 63.
- ⁶Y. Zhao, M. J. Aziz, H.-J. Gossmann, S. Mitha, and D. Schiferl, Appl. Phys. Lett. **74**, 31 (1999).
- ⁷Y. Zhao, M. J. Aziz, H.-J. Gossmann, S. Mitha, and D. Schiferl, Appl. Phys. Lett. **75**, 941 (1999).
- ⁸A. Yu. Kuznetsov, J. Cardenas, D. C. Schmidt, B. G. Svensson, J. Lundsgaard Hansen, and A. Nylandsted Larsen, Phys. Rev. B **59**, 7274 (1999).
- ⁹A. Nylandsted Larsen and P. Kringhøj, Appl. Phys. Lett. **68**, 2684 (1996).
- ¹⁰P. Kringhøj, A. Nylandsted Larsen, and S. Yu. Shirayev, Phys. Rev. Lett. **76**, 3372 (1996).
- ¹¹M. J. Aziz, in *Defects and Diffusion in Silicon Processing*, edited by T. Diaz de la Rubia *et al.*, Mater. Res. Soc. Symp. Proc. No. 469 (Materials Research Society, Warrendale, PA, 1997), p. 37.
- ¹²C. S. Peng, H. Chen, Z. Y. Zhao, J. H. Li, D. Y. Dai, Q. Huang, J. M. Zhou, Y. H. Zhang, C. H. Tung, T. T. Sheng, and J. Wang, J. Cryst. Growth **201/202**, 530 (1999).
- ¹³Y. H. Luo, J. Wan, R. L. Forrest, J. L. Liu, M. S. Goorsky, and K. L. Wang, J. Appl. Phys. **89**, 8279 (2001).
- ¹⁴J. D. Plummer, M. D. Deal, and P. B. Griffin, *Silicon VLSI Technology* (Prentice-Hall, 2000), p. 403.
- ¹⁵M. Petravić, B. G. Svensson, and J. S. Williams, Appl. Phys. Lett. **62**, 278 (1993).
- ¹⁶Bull. Alloy Phase Diagrams **6**, 445 (1985).
- ¹⁷P. M. Fahey, P. B. Griffin, and J. D. Plummer, Rev. Mod. Phys. **61**, 289 (1989).
- ¹⁸S. C. Jain, H. E. Maes, K. Pinaridi, and I. De Wolf, J. Appl. Phys. **79**, 8145 (1996).
- ¹⁹I. Markov, *Crystal Growth for Beginners* (World Scientific, Singapore, 1995).
- ²⁰J. Philibert, *Atom Movements, Diffusion and Mass Transport in Solids* (Editions de Physique, Les Ulis, 1991).
- ²¹H. Mehrer, *Defect and Diffusion Forum* (Scitec Publications, 1996), Vol. 129/130, p. 57.
- ²²A. Antonelli and J. Bernholc, Phys. Rev. B **40**, 10 643 (1989).
- ²³M. J. Aziz, Appl. Phys. Lett. **70**, 2810 (1997).
- ²⁴M. Tang, L. Colombo, J. Zhu, and T. Diaz de la Rubia, Phys. Rev. B **55**, 14 279 (1997).
- ²⁵H. Seong and L. J. Lewis, Phys. Rev. B **53**, 9791 (1996).
- ²⁶M. Werner, H. Mehrer, and H. D. Hochheimer, Phys. Rev. B **32**, 3930 (1985).